Low temperature magnetic properties of geometrically frustrated $Gd_2Sn_2O_7$ and $Gd_2Ti_2O_7$

2003 J. Phys.: Condens. Matter 15 7777

(http://iopscience.iop.org/0953-8984/15/45/016)

INSTITUTE OF PHYSICS PUBLISHING JOURNAL OF PHYSICS: CONDENSED MATTER

J. Phys.: Condens. Matter **15** (2003) 7777–7787 PII: S0953-8984(03)63557-5

Low temperature magnetic properties of geometrically frustrated $Gd_2Sn_2O_7$ and $Gd_2Ti_2O_7$

P Bonville[1], J A Hodges[1], M Ocio[1], J P Sanchez[2], P Vulliet[2], S Sosin[2] and D Braithwaite[2]

[1] CEA, Centre d'Etudes de Saclay, Service de Physique de l'Etat Condensé, 91191 Gif sur Yvette, France
[2] CEA, Centre d'Etudes de Grenoble, Service de Physique Statistique, Magnétisme et Supraconductivité, 38054 Grenoble, France

E-mail: bonville@spec.saclay.cea.fr

Received 13 May 2003
Published 31 October 2003
Online at stacks.iop.org/JPhysCM/15/7777

Abstract

We have examined the low temperature magnetic properties of the geometrically frustrated antiferromagnetic pyrochlores $Gd_2Sn_2O_7$ and $Gd_2Ti_2O_7$ using specific heat, ^{155}Gd Mössbauer, magnetic susceptibility and magnetization measurements. For $Gd_2Sn_2O_7$, the specific heat evidences a single, strongly first order magnetic transition near 1.0 K; in $Gd_2Ti_2O_7$, we confirm the presence of both the transition near 1.0 K and the second transition near 0.75 K. Below 1 K, magnetic irreversibilities are present in both compounds, but their signature (the difference between the FC and ZFC branches) is more marked in $Gd_2Sn_2O_7$. At 0.03 K in each compound, the Mössbauer data show that the four Gd^{3+} of a tetrahedron carry moments of equal sizes and on a frequency scale of 120×10^6 s^{-1} each is oriented perpendicular to the local $\langle 111 \rangle$ direction. In $Gd_2Ti_2O_7$, the Mössbauer data also indicates that the transition at 0.75 K involves a small change in the magnetic structure.

1. Introduction

Interest in geometrically frustrated magnetic systems [1–4] has been stimulated by recent results in the pyrochlores $R_2X_2O_7$ (R^{3+} is a rare earth, X^{4+} a diamagnetic ion) [5–8]. In these compounds, the R^{3+} form a sublattice of corner sharing tetrahedra [9, 10], an arrangement that is particularly prone to frustration [11]. Most of the recent new insight into frustrated systems has arisen from the study of rare earths with Ising behaviour [5–8, 12–14]. Rare earths with planar anisotropy have also been examined [15, 16]. The case $R^{3+} = Gd^{3+}$ is unique since this S-state ion has only a very small intrinsic anisotropy. Villain [1] showed that when such ions form corner sharing tetrahedra and are coupled by an isotropic antiferromagnetic exchange interaction, no magnetic phase transition occurs and as $T \to 0$, the

system remains in a fluctuating collective paramagnetic state. Perturbations such as the dipole–dipole interaction [17, 18], anisotropic exchange or exchange with more distant neighbours may also play a key role and their influence may lead to low temperature properties which differ from those of the collective paramagnet. Specific perturbations clearly do influence the low temperature properties of the Gd pyrochlores since they are known to undergo a magnetic transition near 1 K: it has been evidenced in $Gd_2Sn_2O_7$ by susceptibility measurements [19, 20] and in $Gd_2Ti_2O_7$ by specific heat [17, 21], susceptibility [19] and neutron diffraction [22] measurements.

In this work, we combine specific heat, ^{155}Gd Mössbauer, magnetic susceptibility and magnetization measurements to examine $Gd_2Sn_2O_7$ and $Gd_2Ti_2O_7$. The specific heat measurements evidence a single, strongly first order magnetic transition near 1.0 K in $Gd_2Sn_2O_7$ and confirm the existence of two transitions, near 1.0 K and 0.75 K, in $Gd_2Ti_2O_7$ [21]. In both compounds, the Mössbauer measurements show that, at 0.03 K, each of the four Gd^{3+} moments making up a tetrahedron is oriented perpendicular to the local $\langle 111 \rangle$ direction and is 'static' on a frequency scale of 120×10^6 s^{-1}. In $Gd_2Sn_2O_7$, we have shown previously [23] that spin dynamics with frequencies below this value persists down to very low temperatures (0.03 K). For $Gd_2Ti_2O_7$, we discuss the compatibility of our results with the magnetic structure derived from the neutron diffraction study [22] and we show that our data suggest that the transition near 0.75 K involves a small change in the magnetic structure. In each compound, the low temperature susceptibility shows a magnetic irreversibility which is more marked in $Gd_2Sn_2O_7$ than in $Gd_2Ti_2O_7$. The two isomorphous pyrochlores where the lattice parameters and the average Gd^{3+}–Gd^{3+} interaction strengths are relatively close to each other show a number of common features, but there are some differences between the details of the two behaviours.

2. Samples

The single phase polycrystalline samples of $Gd_2Sn_2O_7$ and $Gd_2Ti_2O_7$ (space group: $Fd\bar{3}m$) were prepared by mixing the constituent oxides and by sintering several times up to 1300 °C with intermediate grinding. The room temperature lattice parameters are 1.046 nm ($Gd_2Sn_2O_7$) and 1.018 nm ($Gd_2Ti_2O_7$). The x-ray background level in $Gd_2Sn_2O_7$ is normal whereas that in $Gd_2Ti_2O_7$ is anomalously high (see section 6).

The point symmetry at the Gd site is $\bar{3}m$ and each Gd^{3+} ion, lying at the vertex of a tetrahedron, has the local $\langle 111 \rangle$ direction as symmetry axis.

3. Specific heat

3.1. $Gd_2Sn_2O_7$

The specific heat measurements obtained using an adiabatic technique and a ^{3}He–^{4}He dilution refrigerator are shown in the left-hand panel of figure 1. There is a single sharp peak at 1.015 K which is superimposed on a broad bump extending up to much higher temperatures. The amplitude of the peak, 120 J K^{-1}/mol Gd, is considerably higher than the mean field value for a second order magnetic transition for $S = 7/2$ (20.4 J K^{-1} mol^{-1}) [24], suggesting the transition is strongly first order. The inset in the left-hand panel of figure 1 shows that only ∼40% of the total magnetic entropy $R \ln 8 = 17.3$ J K^{-1} mol^{-1} Gd is released up to the temperature of the anomaly. Short range correlations are thus present at higher temperatures.

Below ∼0.9 K, the specific heat follows a T^2 dependence (dashed line in the main part of figure 1 (left)). This behaviour contrasts with the T^3 dependence which is characteristic

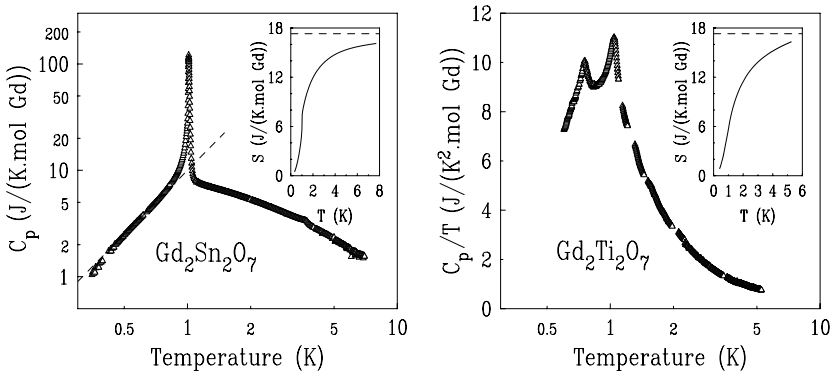

Figure 1. Left: thermal variation of the specific heat for $Gd_2Sn_2O_7$; the dashed line represents the law $C_p = \alpha T^2$, with $\alpha = 10$ J K^{-3} mol^{-1} Gd; right: thermal variation of the specific heat divided by the temperature for $Gd_2Ti_2O_7$. The insets show the variation in entropy and the dashed lines represent $R \ln 8 = 17.3$ J K^{-1} mol^{-1} Gd, the total entropy associated with a spin $S = 7/2$.

of a standard 3D antiferromagnet and which has been observed, for example, in the antiferromagnetic pyrochlore $Er_2Ti_2O_7$ [25]. In general, a T^2 dependence implies a density of states which increases linearly in energy. It is predicted to occur in the case of a 2D Heisenberg antiferromagnet [26] and it has been evidenced in a layered antiferromagnet [27], in a quasi-2D spin glass [28] and for a type A antiferromagnet with an assumed particular anisotropic dispersion relation [29]. These cases all involve systems having a local anisotropy. It is thus possible that the T^2 behaviour observed in $Gd_2Sn_2O_7$ could be linked to an anisotropy in the exchange interaction such as that evidenced (in $Gd_2Ti_2O_7$) by electron spin resonance measurements [30].

3.2. $Gd_2Ti_2O_7$

The specific heat measurements obtained using an adiabatic technique and a ^{3}He refrigerator are shown in the right-hand panel of figure 1. There is a peak at 1.045 K and a second peak at 0.75 K as reported previously [21]. The amplitudes of the peaks are an order of magnitude lower than the peak in $Gd_2Sn_2O_7$. Approximately 20% and 35% of the total magnetic entropy of $R \ln 8$ is respectively released up to the temperatures of the two peaks and, as shown by the inset in the right-hand panel of figure 1, short range order is present at temperatures above that of the upper peak. The specific heat data indicates that the upper peak does not correspond to a transition which is strongly first order. However, there is some indication (section 5.2) that this transition does possess some weak first order character.

4. ^{155}Gd Mössbauer measurements

4.1. $Gd_2Sn_2O_7$

Selected ^{155}Gd Mössbauer spectra ($I_g = 3/2$, $I_e = 5/2$, $E_\gamma = 86.5$ keV, 1 mm s$^{-1} \equiv$ 69.8 MHz, source: Sm^*Pd_3) are shown in panel (a) of figure 2. Down to 1.1 K, a quadrupole hyperfine interaction is observed, in agreement with previous measurements at 4.2 K [31]. The quadrupolar interaction (splitting) is -4.0 mm s^{-1}, with the sign obtained from the data below 1.0 K. An additional magnetic hyperfine interaction appears suddenly between 1.10 and 1.05 K (see the corresponding spectra in figure 2 panel (a)). Below 1.05 K the data analysis provides

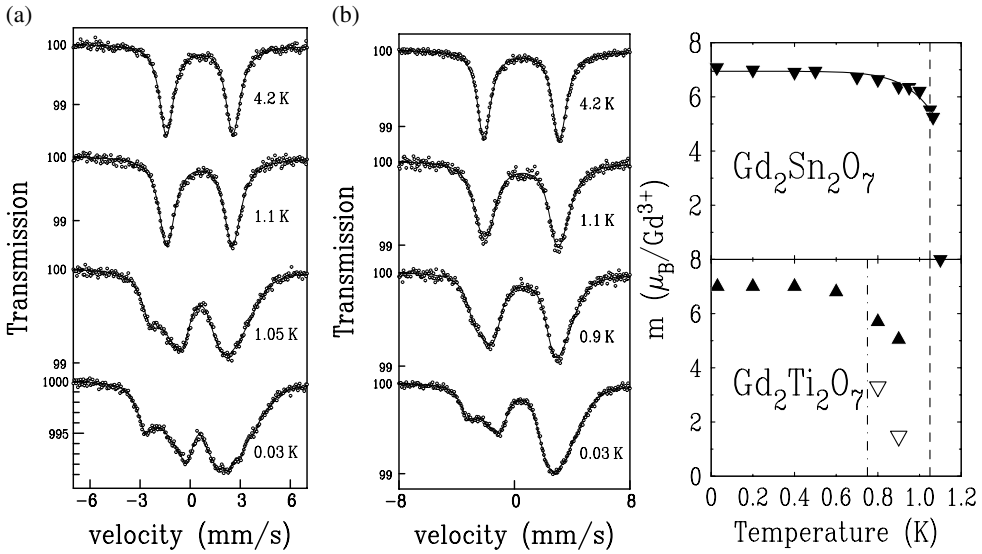

Figure 2. ^{155}Gd Mössbauer absorption spectra for $Gd_2Sn_2O_7$ (left-hand panel, (a)) and $Gd_2Ti_2O_7$ (middle panel, (b)) as a function of temperature. Thermal variation of the Gd^{3+} magnetic moment in $Gd_2Sn_2O_7$ (right-hand panel, top) and $Gd_2Ti_2O_7$ (right-hand panel, bottom) obtained from the ^{155}Gd Mössbauer measurements. The dashed line marks the position of the maxima of the specific heat peaks (∼1.05 K) in the two compounds. The chain line marks the position of the second transition in $Gd_2Ti_2O_7$ (∼0.75 K). Above this temperature, two different Gd^{3+} moments are evidenced (full and open triangles) (see text).

the size of the hyperfine field and its direction relative to the principal axis of the electric field gradient (EFG) tensor, which is the local ⟨111⟩ axis. At each temperature, the Mössbauer lineshape is well described by a unique hyperfine field which is oriented 90(5)° to the principal axis of the EFG. Since the Gd^{3+} spontaneous magnetic moment $m(T)$ is proportional to the hyperfine field $H_{\rm hf}(T)$, this shows that at each temperature the four moments of a tetrahedron have a common size and each is perpendicular to the local ⟨111⟩ axis. The magnetic moment value $m(T)$ is obtained from the scaling law

$$m(T) = m_0 \frac{H_{\rm hf}(T)}{H_{\rm hf}(0)}, \tag{1}$$

where m_0 is the saturated low temperature Gd^{3+} moment (7 μ_B), and $H_{\rm hf}(0)$ is the saturated hyperfine field value (29.9 T). The thermal variation of $m(T)$ is given in the top part of the right-hand panel of figure 2. The moment shows a smooth decrease as the temperature is raised from 0.03 to 1.065 K. At 1.065 K, it amounts to 75% of the saturated value and then drops abruptly to zero at 1.1 K. A second order transition, with a very 'square' variation of the order parameter, cannot in principle be discarded. However, both evidences of a very high specific heat jump and of a very steep moment decrease at T_N point to a magnetic transition with a strong first order character in $Gd_2Sn_2O_7$. The observed hyperfine fields (and the associated correlated magnetic moments) are 'static' on the ^{155}Gd hyperfine Larmor frequency scale of $\sim 120 \times 10^6$ s^{-1}. The fluctuations of the moments evidenced as $T \to 0$ in [23] thus occur at a rate which is lower than this value. They link directions which are perpendicular to each local ⟨111⟩ axis.

4.2. $Gd_2Ti_2O_7$

Selected ^{155}Gd Mössbauer spectra are shown in the middle panel (b) of figure 2. At 4.2 K, a quadrupole hyperfine interaction [31] is visible, with a quadrupole splitting -5.6 mm s^{-1}. As the temperature is lowered from 4.2 to 1.1 K (i.e. in the temperature range just above that of the upper specific heat peak), each of the two absorption lines broadens considerably. We attribute this broadening to the slowing down of the fluctuations of the short range correlated Gd^{3+} magnetic moments. No comparable line broadening occurs in $Gd_2Sn_2O_7$, showing that for this compound, in the equivalent temperature range, the fluctuation rate of the short range correlated moments does not slow down enough to enter the ^{155}Gd frequency window. This line broadening acts to mask the magnetic transition near 1.0 K. Well below this temperature, the line shape evidences the characteristic structure associated with combined quadrupole and magnetic hyperfine interactions.

Up to 0.6 K, the spectra are very satisfactorily fitted with a single hyperfine field perpendicular to the principal axis of the EFG, like in $Gd_2Sn_2O_7$. This means that the four Gd^{3+} ions of a tetrahedron carry moments which have a common size and each is perpendicular to the local $\langle 111 \rangle$ axis. The moments were obtained from the hyperfine field values using the scaling law (1), with a measured saturated hyperfine field $H_{\rm hf}(0) = 28.3$ T, slightly smaller than in $Gd_2Sn_2O_7$. Their thermal variation is shown in the bottom part of the right-hand panel of figure 2.

At low temperatures, the Gd^{3+} moment is essentially temperature independent whereas at 0.8 K and above it decreases with increasing temperature. At 0.8 K and above, the Mössbauer analysis indicates that the four moments of a tetrahedron are no longer identical. The evidence for this is presented later in this section. No reliable values for the moments could be obtained above 0.9 K due to the influence of the dynamical broadening of the Mössbauer lines. The thermal variation of the Gd^{3+} moment (the average value at 0.8 K and above) is similar to that obtained from the neutron diffraction measurements [32].

The neutron diffraction measurements [22] showed that the low temperature magnetic structure has a propagation vector $\mathbf{k} = (\frac{1}{2}, \frac{1}{2}, \frac{1}{2})$, in agreement with the predictions of [17]. The magnetic structure was considered in terms of a set of two dimensional *kagomé* sheets (the $\{111\}$ planes) linked by a plane of 'interstitial' Gd ions. The proposed low temperature (0.05 and 0.5 K) structure (model (iii) in [22]) consisted of a triangular array of co-planar moments lying in the *kagomé* sheets, with each moment perpendicular to the local $\langle 111 \rangle$ axis and with no visible moment on the fourth site of a tetrahedron lying in the 'interstitial' planes. The neutron diffraction analysis cannot determine whether the derived moment in the 'interstitial' plane vanishes because of directional disorder ('static' hypothesis) or whether it vanishes because the moments are fluctuating too rapidly to be detected ('dynamic' hypothesis). The Mössbauer measurements are able to shed light on this aspect. Figure 3 shows the data fits obtained respectively with the 'static' and the 'dynamic' hypotheses. In the 'static' hypothesis, the spectrum is fitted to a single magneto-quadrupolar hyperfine pattern, with the hyperfine field perpendicular to the principal axis of the EFG tensor. In the 'dynamic' hypothesis, the spectrum is fitted to the sum of a magneto-quadrupolar pattern as above, with relative weight 3/4, and of a quadrupolar pattern (i.e. with zero hyperfine field), with relative weight 1/4. It is clear that the comparison eliminates the 'dynamic' hypothesis and shows (as reported above) that the fourth site of a tetrahedron carries a moment which has the same size and local direction (perpendicular to the local $\langle 111 \rangle$ axis) as the other three. In addition, the fact that the 'interstitial' moment remains important up to at least 0.6 K shows that this site experiences a sizeable molecular field. It is not clear how the structure (iii) of [22] could give rise to this situation since the moments in the *kagomé* planes appear to show inversion symmetry around

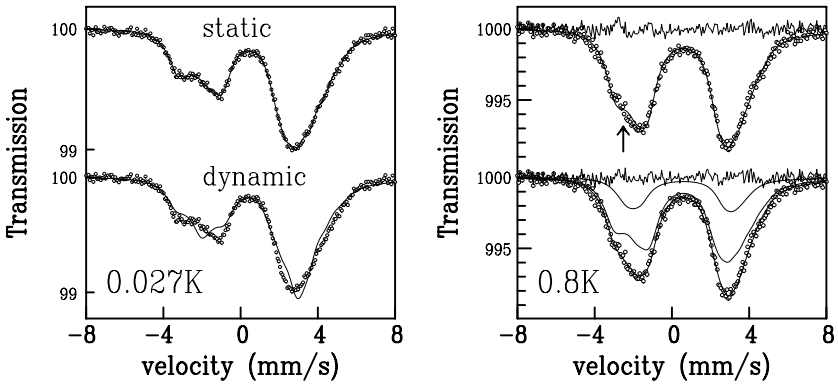

Figure 3. Fits of the ^{155}Gd Mössbauer spectra in $Gd_2Ti_2O_7$. Left: at 0.027 K in terms of model (iii) for the magnetic structure of [22] assuming a static (top) and dynamic (bottom) disorder for the 'interstitial' Gd moment (see text); right: at 0.8 K with two fitting hypotheses: a single hyperfine field perpendicular to the principal axis of the EFG (top), and two subspectra (bottom), one with 75% relative intensity having its hyperfine field perpendicular to the principal axis of the EFG, the other (25%) having a smaller hyperfine field oriented at 60(10)° to the principal axis of the EFG. The difference between experimental and calculated curves is shown for each hypothesis.

the interstitial site such that the planar antiferromagnetic structure on the *kagomé* sheets leads to a zero mean field at the interstitial site. It would be of interest to examine whether this structure could give rise to a non-zero molecular field at the fourth site if the influence of higher order bilinear terms in the exchange interaction is taken into account.

We now turn to the evidence suggesting there is a change in the magnetic structure between 0.6 and 0.8 K (i.e. on crossing the temperature of the specific heat transition near 0.75 K). When the data at 0.8 and 0.9 K are fitted with the hypothesis which is appropriate at 0.6 K and below (four equivalent sites), there occurs a slight but clear misfit at both temperatures. This misfit is indicated by the arrow in the top part of the right-hand panel of figure 3. To remove this misfit, it is necessary to relax the condition that the four moments of a tetrahedron have identical characteristics. A much better fit (bottom part of the right-hand panel of figure 3) is obtained if three of the sites retain an orientation perpendicular to the local $\langle 111 \rangle$ axis ($\theta = 90°$, $m = 5.7\ \mu_B$) and the fourth site has a tilted and different sized moment ($\theta \sim 60°$, $m = 3.3\ \mu_B$). The improvement this two-subspectra assumption brings to the fit can be seen by the difference spectra shown in the right-hand panel of figure 3. The two-subspectra fit also leads to an improvement of the data fit at 0.9 K. In terms of the magnetic structure, this could correspond to unchanged spin orientations in the *kagomé* sheets, but to 'interstitial' Gd moments which now point out of the plane, for instance towards a $\langle 001 \rangle$ axis ($\theta = 54.7°$). However, this fitting solution is not the only one possible and the detailed magnetic structure in the phase above 0.75 K will have to be determined by neutron diffraction experiments. Our analysis suggests that a multi-k magnetic structure can be ruled out below 0.75 K, because this implies a non-zero moment component along a $\langle 111 \rangle$ direction [22] contrary to our findings. However, above 0.75 K, the Mössbauer data indicates that a multi-k structure is possible.

Although $Gd_2Sn_2O_7$ and $Gd_2Ti_2O_7$ share the common characteristic that in the low temperature limit the four moments of a tetrahedron are perpendicular to the local $\langle 111 \rangle$ axis, this does not entail that the magnetic structures are the same in the two compounds. This is supported by the μSR measurements performed at 0.02 K, which show different oscillating depolarization signals for the two compounds (see [33] for $Gd_2Sn_2O_7$ and [34] for $Gd_2Ti_2O_7$). Direct information concerning the magnetic structure of $Gd_2Sn_2O_7$ will be provided by our planned neutron diffraction measurements on isotopically enriched samples.

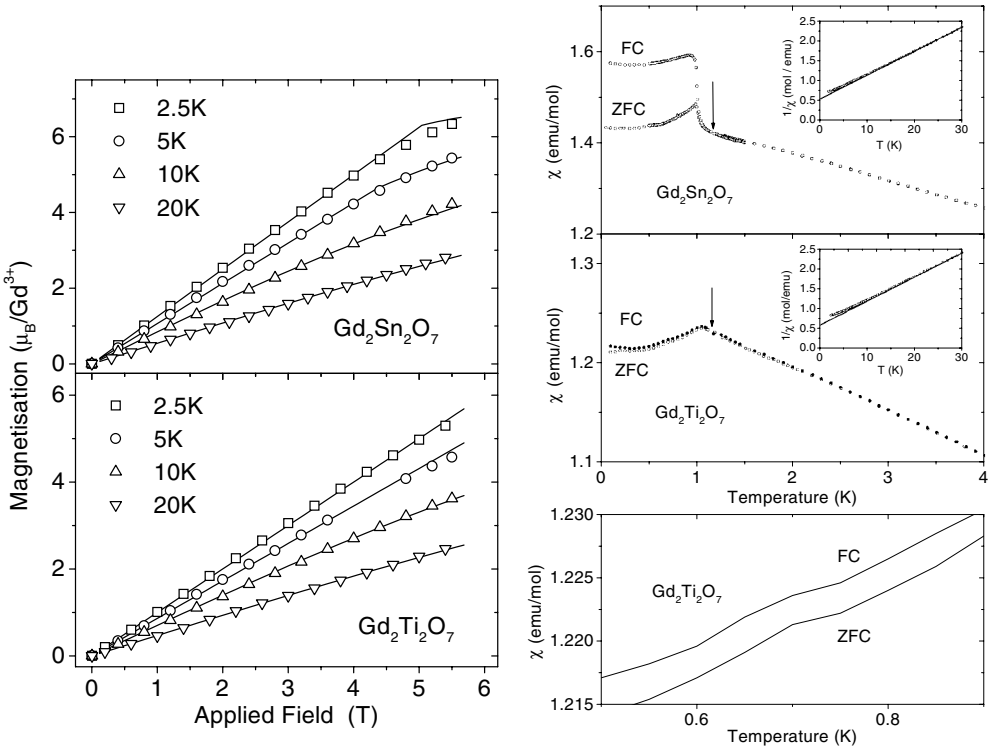

Figure 4. Left: the dependence of the magnetization on applied field and temperature for $Gd_2Sn_2O_7$ (upper part) and $Gd_2Ti_2O_7$ (lower part) fitted with a molecular field model. Right (upper part): the static magnetic susceptibility and inverse magnetic susceptibility (insets) per formula unit for $Gd_2Sn_2O_7$ and $Gd_2Ti_2O_7$ in the FC and ZFC configurations. The arrows show the temperatures around which no data points could be obtained (see text). The straight line in each of the insets is the extrapolated high temperature Curie–Weiss dependence. Right (lower part): the static magnetic susceptibility in $Gd_2Ti_2O_7$ evidencing a weak anomaly in both the FC and ZFC variations near 0.7 K; the lines shown join the data points which have been omitted.

5. Bulk magnetic measurements

5.1. Magnetization and susceptibility above 1.4 K

The measurements were made using a commercial SQUID magnetometer. At all temperatures, the magnetization in each compound shows an almost linear dependence on applied field, and even at 2.5 K under 5.5 T the moment falls short of the saturated value of 7.0 μ_B per Gd^{3+} (left-hand panel of figure 4). The data thus evidence the presence of relatively strong antiferromagnetic inter-ionic interactions. Their strength can be estimated within a molecular field approach. As an approximation, we use a two-sublattice self-consistent calculation with an isotropic antiferromagnetic coupling constant. Although this model represents a simplification of the real situation where there are four and not two different Gd^{3+} sites and where the total inter-ionic interactions may be anisotropic [30], it does provide the average size of the inter-ionic coupling. As shown in the left-hand panel of figure 4, the field and temperature dependence of the magnetization is well reproduced by this model, which provides an average coupling constant of $-0.45(10)$ ($Gd_2Sn_2O_7$) and $-0.6(0.1)$ T/μ_B($Gd_2Ti_2O_7$).

In each compound, the susceptibility shows Curie–Weiss behaviour above $\sim$15 K (insets in the right-hand panel of figure 4). We obtain paramagnetic Curie temperatures

$\theta_p = -8.6(1)$ ($Gd_2Sn_2O_7$) and $-9.9(1)$ K ($Gd_2Ti_2O_7$) (antiferromagnetic interactions), close to previously reported values [17, 19, 20, 35]. Within the molecular field model, these values correspond to average coupling constants of $-0.6(0.1)$ ($Gd_2Sn_2O_7$) and $-0.7(0.1)T/\mu_B$ ($Gd_2Ti_2O_7$). To within experimental error, these are coherent with the coupling constants obtained from the magnetization data. Both the magnetization and susceptibility data indicate that the total coupling strength is 15–30% lower in $Gd_2Sn_2O_7$ than in $Gd_2Ti_2O_7$, in line with the larger lattice constant in $Gd_2Sn_2O_7$. The change in lattice constant influences the sizes of both the average exchange and dipole–dipole coupling. It seems likely however that in $Gd_2Sn_2O_7$ the dipole–dipole coupling amounts to approximately 20% of the average exchange coupling, as it does in $Gd_2Ti_2O_7$ [17].

5.2. dc magnetic susceptibility down to 0.1 K

The measurements were obtained with a field of 10 mT using a home-built SQUID magnetometer coupled to a ^{3}He–^{4}He dilution refrigerator.

In each compound the magnetic susceptibility shows anomalies close to 1 K (the right-hand panel of figure 4 (top)). As the temperature is lowered in $Gd_2Sn_2O_7$, there is a sharp upturn in the susceptibility followed by maxima in both the FC and ZFC dependences and a marked irreversibility. In $Gd_2Ti_2O_7$, there is no upturn and the size of the irreversibility is an order of magnitude smaller than in $Gd_2Sn_2O_7$.

In $Gd_2Sn_2O_7$, we found that with the standard temperature controller of the susceptibility setup, it was not possible to stabilize the temperature of the sample within a small temperature interval whose centre is indicated by the arrow in the right-hand panel of figure 4 (top). Consequently, there are no data points in this interval on the figure. We link this behaviour to the presence of a latent heat associated with the strong first order transition evidenced by the specific heat and Mössbauer measurements. The same phenomenon was observed during the susceptibility measurements in $Gd_2Ti_2O_7$, at a temperature around that indicated by the arrow on figure 4 right (top). We note that there are also no data points in an equivalent small temperature interval near 1 K in the ac susceptibility data of figure 3 of [17], nor in the dc susceptibility data of figure 2 of [19]. By analogy with $Gd_2Sn_2O_7$, we interpret this behaviour to indicate that the transition in $Gd_2Ti_2O_7$ also involves a latent heat and consequently that it shows some first order character. It is clear, however, that this character is quite weak since there is no evidence from the specific heat data of any first order behaviour.

The bottom part of the right-hand panel of figure 4 shows that in $Gd_2Ti_2O_7$ there is a small anomaly in both the FC and ZFC susceptibilities at the temperature of the lower specific heat peak (0.75 K). No anomaly was reported in the previous ac magnetic susceptibility measurements [21]. The transition marked by this specific heat peak is thus clearly of magnetic (rather than say crystallographic) origin. This is confirmed by the appearance of a slight change in the characteristics of the Mössbauer derived Gd^{3+} magnetic moments (section 4.2).

6. Summary and discussion

We have established a number of the low temperature properties of the two isomorphous antiferromagnetic pyrochlores $Gd_2Sn_2O_7$ and $Gd_2Ti_2O_7$ where there are only modest differences between the lattice parameters and between the average strengths of the Gd^{3+}–Gd^{3+} interactions.

On comparing the two sets of results, it is clear that the two compounds share a number of common characteristics although there are differences between the details of the two behaviours. The only major phenomenon that is not common to the two compounds is the

second specific heat peak near 0.75 K, which is only present in $Gd_2Ti_2O_7$. The phenomenon associated with this peak does not then appear to be a generic characteristic of AF coupled Gd^{3+} ions on the pyrochlore lattice.

Each compound exhibits a characteristic property of frustrated systems: the magnetic transition takes place at a temperature which is very much lower than that corresponding to the strength of the magnetic coupling. The transitions near 1.0 K take place at closely comparable temperatures (the maximum in the specific heat peak in $Gd_2Ti_2O_7$ lies $\sim$3% higher than that in $Gd_2Sn_2O_7$) whereas the average Gd^{3+}–Gd^{3+} coupling is 15–30% higher in $Gd_2Ti_2O_7$ than in $Gd_2Sn_2O_7$. The transition temperature does not then scale with the average coupling strength.

The transition near 1.0 K has a complex character. Its main feature is that it is strongly first order in $Gd_2Sn_2O_7$ and there is some evidence of weak first order behaviour in $Gd_2Ti_2O_7$. Although the pyrochlore lattice is capable of displaying a first order magnetic transition which does not involve long range magnetic ordering [15], the transition at 1 K in $Gd_2Sn_2O_7$ is associated with the onset of long range ordering [33] as it is in $Gd_2Ti_2O_7$ [22]. The magnetic structure however is probably different in the two cases.

In $Gd_2Sn_2O_7$, the correlated Gd^{3+} moments retain dynamic character as $T \rightarrow 0$ [23]. The evidenced spin fluctuations link directions which are perpendicular to the local $\langle 111 \rangle$ axes and they occur at a frequency below 120×10^6 s^{-1}. Although frustration does not prevent the occurrence of a magnetic transition to a (presumably) long range ordered state, it acts to maintain the collective fluctuations of the moments (between specific spin directions) as $T \rightarrow 0$. The persisting low temperature spin dynamics provides direct evidence for zero point excitations and for a finite zero point density of states. The observed T^2 dependence of the specific heat indicates that the density of states of the excitations also contains a part with a density which increases linearly with energy. These findings contrast with the theoretical predictions of the density of states for the Heisenberg pyrochlore antiferromagnet, where although the density of states also remains finite at zero energy, at higher energies it contains a part which is independent of energy [36]. In $Gd_2Ti_2O_7$, the Mössbauer measurements do not provide any direct indication that the correlated Gd^{3+} moments retain dynamic character as $T \rightarrow 0$ [23], but they do not exclude this possibility either.

A good understanding of the role of perturbations will be primordial to the full comprehension of the experimental properties of the frustrated pyrochlores. In addition to the possible intrinsic perturbations (dipole coupling, exchange anisotropy, further neighbour coupling, etc), it is possible that extrinsic perturbations also play a role. For example, some elements suggest that $Gd_2Ti_2O_7$ is less crystallographically homogeneous than $Gd_2Sn_2O_7$. First, we observe that the fitted Mössbauer linewidths are systematically broader in $Gd_2Ti_2O_7$, suggesting that it has a higher level of crystallographic inhomogeneity, and second, we observe that in all our samples of $Gd_2Ti_2O_7$ (including a crushed single crystal sample), the x-ray patterns evidence sharp diffraction lines but they also show anomalously high background levels. These anomalous levels were reported previously [37] and in fact they were also encountered in the $R_2Ti_2O_7$ with $R^{3+} = Eu^{3+}$, Gd^{3+}, Sm^{3+} and Nd^{3+} [37], that is, in the titanates where the rare earth ion has a medium or a small radius. The anomalous background which is not present in $Gd_2Sn_2O_7$ can be linked to crystallographic inhomogeneities. At present, the precise origin of these inhomogeneities (site inversion, disorder, vacancies) is not known. The presence of inhomogeneities in $Gd_2Ti_2O_7$ and their absence in $Gd_2Sn_2O_7$ may also explain why the different anomalies that are common to the two compounds are more sharply defined in $Gd_2Sn_2O_7$.

Finally, in table 1, we summarize some of the key parameters obtained for the two pyrochlores studied here and we compare, where possible, with the equivalent data for the isomorphous pyrochlores containing the heavier rare earths (R). The case R = Tm is not included since the Tm^{3+} ground state is a non-magnetic singlet [38]. More data is presently

Table 1. Some properties of $Gd_2Sn_2O_7$ and $Gd_2Ti_2O_7$, together with the comparable data for the isomorphous pyrochlores containing the heavier rare earths. θ_p: the paramagnetic Curie temperature (a negative sign corresponds to a net antiferromagnetic interaction); T_{mag}: the temperature of the magnetic transition (if any); μ (μ_B): the size of the rare earth magnetic moment as $T \to 0$; direction: the local direction of a (short or long) range correlated moment relative to its appropriate symmetry axis; LRO: existence of long range magnetic order; SD: existence of rare earth moment spin dynamics. Each temperature in brackets represents the relevant lowest measurement temperature. (Note: the numbers in square brackets link to the reference list at the end of the paper.)

	θ_p (K)	T_{mag} (K)	μ (μ_B)	Direction	LRO	SD
$Gd_2Ti_2O_7$	−9.9[a]	0.75, 1.02 [21][a]	7.0	$\perp \langle 111 \rangle$[a]	Yes [22]	Yes(0.03 K) [34]
$Gd_2Sn_2O_7$	−8.6[a]	1.05[a]	7.0	$\perp \langle 111 \rangle$[a]	Yes [33]	Yes(0.03 K) [33]
$Tb_2Ti_2O_7$	−19 [7]	<0.07 [7]	9.0[b]	$\parallel \langle 111 \rangle$[b]	No(0.07 K) [7][c]	Yes(0.07 K) [7]
$Tb_2Sn_2O_7$	−11.1 [35]	<1.4 [39]	—	—	No(1.4 K) [39]	—
$Dy_2Ti_2O_7$	+0.5 [6]	<0.06 [40, 41]	∼10 [42]	$\parallel \langle 111 \rangle$[b]	No(0.05 K) [40]	Yes(0.25 K)[e]
$Dy_2Sn_2O_7$	−0.7 [35][d]	<1.8 [35]	—	—	—	—
$Ho_2Ti_2O_7$	+1.9 [5]	<0.05 [12]	10.0[b]	$\parallel \langle 111 \rangle$[b]	No(0.05 K) [12]	Yes(0.05 K) [12]
$Ho_2Sn_2O_7$	+1.8 [43]	<0.4 [44]	—	—	—	—
$Er_2Ti_2O_7$	−22 [45][f]	1.2 [25, 45]	3.0 [25]	—	Yes [25]	—
$Er_2Sn_2O_7$	−18.0 [35][f]	<1.8 [35]	—	—	—	—
$Yb_2Ti_2O_7$	+0.7 [46]	0.24 [15]	1.15 [15]	44° to $\langle 111 \rangle$ [15]	No (0.04 K) [15][h]	Yes(0.04 K) [15]
$Yb_2Sn_2O_7$	+0.5[g]	0.12[g]	1.15[g]	60° to $\langle 111 \rangle$[g]	No (0.05 K) [47]	Yes(0.05 K) [47]

[a] Present work.
[b] Approximate value expected from the ground state wavefunction.
[c] LRO is induced by an external pressure, see [48].
[d] The value will become positive if demagnetization effects are taken into account.
[e] Indirect evidence, see [23].
[f] This value may be lower if the influence of low lying crystal field levels is taken into account.
[g] Our unpublished results.
[h] The short range correlations evidenced by neutron diffraction are antiferromagnetic [33].

available concerning the Ti-based pyrochlores than concerning those containing Sn. When results are available in both cases (for example our results for R = Gd and Yb) there is a measure of similarity between the two sets of data. It is likely that this similarity will extend to the other rare earths.

We note that a magnetic transition occurs only in compounds where the rare earth is a Kramers ion. All such compounds show a magnetic transition with the exception of the case R = Dy. The influence of the non-Kramers nature of the rare earth (Tb^{3+}, Ho^{3+}) on the low temperature magnetic properties has yet to be examined in detail. The existence of a magnetic transition does not automatically entail the existence of long range magnetic order: for R = Gd the transition involves long range order, but for R = Yb the transition does not involve long range order, but an abrupt slowing down of the spin fluctuations. In all cases, whether or not there is a magnetic transition, the rare earth moments evidence persisting spin dynamics as $T \to 0$. This appears to be a generic feature of the rare earth pyrochlores.

Acknowledgments

We thank Anne Forget for preparing the polycrystalline samples and Nadine Genand-Riondet for technical assistance.

References

[1] Villain J 1979 *Z. Phys.* B **33** 31
[2] Kinney W I and Wolf W P 1979 *J. Appl. Phys.* **50** 2115
[3] Diep H T (ed) 1994 *Magnetic Systems with Competing Interactions* (Singapore: World Scientific)
[4] Schiffer P and Ramirez A P 1996 *Comment. Condens. Matter. Phys.* **18** 21
[5] Harris M J *et al* 1997 *Phys. Rev. Lett.* **79** 2554
[6] Ramirez A P *et al* 1999 *Nature* **399** 333
[7] Gardner J S *et al* 1999 *Phys. Rev. Lett.* **82** 1012
[8] den Hertog B C and Gingras M J P 2000 *Phys. Rev. Lett.* **84** 3430
[9] Subramanian M A, Aravamudan G and Subba Rao G V 1983 *Prog. Solid State Chem.* **15** 55
[10] Greedan J E 1992 *Landolt–Börnstein New Series* Group III, vol 27g (Berlin: Springer) pp 87–123
[11] Moessner R 2001 *Can. J. Phys.* **79** 1283
[12] Harris M J *et al* 1998 *J. Magn. Magn. Mater.* **177–181** 757
[13] Matsuhira K, Hinatsu Y and Sakakibara T 2001 *J. Phys.: Condens. Matter* **13** L737
[14] Bramwell S T *et al* 2001 *Phys. Rev. Lett.* **87** 047205
[15] Hodges J A *et al* 2002 *Phys. Rev. Lett.* **88** 077204
[16] Bramwell S T, Gingras M J P and Reimers J N 1994 *J. Appl. Phys.* **75** 5523
[17] Raju N P *et al* 1999 *Phys. Rev.* B **59** 14489
[18] Palmer S E and Chalker J T 2000 *Phys. Rev.* B **62** 488
[19] Luo G, Hess S T and Corruccini L R 2001 *Phys. Lett.* A **291** 306
[20] Matsuhira K, Hinatsu Y, Tenya K, Amitsuka H and Sakakibara T 2002 *J. Phys. Soc. Japan* **71** 1576
[21] Ramirez A P, Shastry B S, Hayashi A, Krajewski J J, Huse D A and Cava R J 2002 *Phys. Rev. Lett.* **89** 067202
[22] Champion J D M, Wills A S, Fennell T, Bramwell S T, Gardner J S and Green M A 2001 *Phys. Rev.* B **64** 140407(R)
[23] Bertin E, Bonville P, Bouchaud J P, Hodges J A, Sanchez J P and Vulliet P 2002 *Eur. Phys. J.* B **27** 347
[24] Stanley H E 1971 *Introduction to Phase Transitions and Critical Phenomena* (Oxford: Clarendon)
[25] Champion J D M *et al* 2003 *Phys. Rev.* B **68** 020401(R)
[26] Kubo R 1952 *Phys. Rev.* **87** 568
[27] Wills A S, Harrison A, Mentink S A M, Mason T E and Tun Z 1998 *Europhys. Lett.* **42** 325
[28] Ramirez A P, Espinosa G P and Cooper A S 1990 *Phys. Rev. Lett.* **64** 2070
[29] Woodfield B F, Wilson M L and Byers J M 1997 *Phys. Rev. Lett.* **78** 3201
[30] Hassan A K, Lévy L P, Darie C and Strobel P 2003 *Phys. Rev.* B **67** 214432
[31] Cashion J D, Prowse D B and Vas A 1973 *J. Phys. C: Solid State Phys.* **6** 2611
[32] Bramwell S T, Harris M J and Champion J D M 1999 *ISIS Experimental Report* RB 10394 Rutherford Appleton Laboratory
[33] Bonville P *et al* 2003 *Proc. 38th Zakopane School of Physics*
Bonville P *et al* 2003 *Preprint* cond-mat/0306470
[34] Hodges J A *et al* 2002 *Paul Scherrer Institute Scientific Report* RA-01-15
[35] Bondah-Jagalu V and Bramwell S T 2001 *Can. J. Phys.* **79** 1381
[36] Moessner R and Chalker J T 1998 *Phys. Rev.* B **58** 12049
[37] Knop O, Brisse F and Castelliz F 1969 *Can. J. Chem.* **47** 971
[38] Zinkin M P, Harris M J, Tun Z, Cowley R A and Wanklyn B M 1966 *J. Phys.: Condens. Matter* **8** 193
[39] Mirebeau I 2002 private communication
[40] Fukazawa F *et al* 2002 *Phys. Rev.* B **65** 054410
[41] Fennell T *et al* 2001 *Preprint* cond-mat/0107414
[42] Almog A, Bauminger E R, Levy A, Nowik I and Ofer S 1973 *Solid State Commun.* **12** 693
[43] Matsuhira K, Hinatsu Y, Tenya K and Sakakibara T 2000 *J. Phys.: Condens. Matter* **12** L649
[44] Kadowaki H, Ishii Y, Matsuhira K and Hinatsu Y 2001 *Preprint* cond-mat/0107278
[45] Blote H W J, Wielinga R F and Huiscamp W J 1969 *Physica* **43** 549
[46] Hodges J A, Bonville P, Forget A, Rams M, Królas K and Dhalenne G 2001 *J. Phys.: Condens. Matter* **13** 9301
[47] Dalmas P *et al* 2003 *ISIS Report* RB 13677
[48] Mirebeau I *et al* 2002 *Nature* **420** 54